Eng. & Tech. Journal, Vol. 29, No.9, 2011

Determination of the Adequate Thickness of Granular Subbase Beneath Foundations

Dr.Mohammed Y. Fattah Dr. Falah H. Rahil*
& Mohammed A. Turki*

Received on: 26 /10 / 2010
Accepted on: 2 / 6 / 2011

Abstract

Where the native soils have poor structural qualities or are expansive, the soil investigation report may recommend importation of soils better suited to providing a subbase for structures. This requires considering two soil layers in bearing capacity calculations.

Calculation of the ultimate bearing capacity of shallow footing on a two layered system of soil depends on the pattern of the failure surface that develops below the footing. For a weak clay layer overlaid by a top dense sand layer, previous studies assumed that the failure surface is a punching shear failure through the upper sand layer and Prandtl's failure mode in the bottom weak clay layer.

In this paper, the bearing capacity of subbase layer underneath by a soft clay layer is investigated. The properties of the subbase material are measured in the laboratory. Design charts were obtained which can be used to select the suitable thickness of the subbase layer for a design allowable bearing capacity.

Keywords: Bearing capacity, granular subbase, thickness, soft clay.

تحديد السمك المناسب لطبقة الحصى الخابط (السبيس) تحت الأسس

الخلاصة

عندما تكون التربة المقترح تنفيذ الأساس عليها ضعيفة أو انتفاخية فان تقرير تحريات التربة يمكن أن يقترح استبدال التربة بطبقة من الحصى الخابط ذات مواصفات أفضل. يتطلب ذلك اعتماد طبقتين من التربة لتحديد قابلية تحمل التربة. يعتمد حساب قابلية التحمل القصوى للأسس الضحلة المنفذة على طبقتي تربة على شكل الفشل الذي يحدث أسفل الأساس. اذ يفترض العديد من الدراسات السابقة شكل الفشل لتربة طينية ضعيفة أسفل تربة رملية قوية من نوع فشل ثقب القص (Punching shear failure) خلال الطبقة الرملية العليا و يتحقق شكل سطح الانزلاق لبراندتل في طبقة الطين الضعيفة السفلى.

في هذا البحث تم التحري عن قابلية التحمل لطبقة الحصى الخابط المشيدة على طبقة طينية ضعيفة حيث تم تحديد خواص الحصى الخابط مختبريا. و تم الحصول على مرتسمات تصميمية يمكن من خلالها تحديد السمك المناسب لطبقة الحصى الخابط لقابلية التحمل المسموح بها تصميميا.

Introduction

The function of a foundation is to transfer the load of the superstructure to the underlying soil formation without overstressing the soil. The soil must be capable of carrying the load for structure(s) placed upon it without shear failure and with the resulting settlement being tolerable for that structure. Many investigations on the subject of ultimate bearing capacity have been carried out during the past century.

* Building and Construction Engineering Department, University of Technology/Baghdad

https://doi.org/10.30684/etj.29.9.18
2412-0758/University of Technology-Iraq, Baghdad, Iraq

Subsequently, numerous proposals have been advanced regarding considerations, criteria, and procedures for evaluation of the ultimate bearing capacity of soils. Among the very early contributors were Prandtl (1921) who developed a solution for a surface strip footing over a perfectly plastic cohesive-frictional weightless half-space. Reissner (1924) extended the solution of Prandtl to include the effect of a uniform surcharge load on the resistance of penetration of ultimate applied load. Since real soils possess weight, Terzaghi (1943) was the first to introduce the concept of ultimate bearing capacity and presented a comprehensive theory for the evaluation of such capacity of shallow foundations. Subsequently, the bearing capacity theory went through many modifications to account for different features such as foundation shape, load inclination, ground slope, nonsymmetrical loads, and water table. The general bearing capacity theories proposed by Meyerhof (1963), Hansen (1970), Vesic (1973) and others are now routinely used in foundation design.

The bearing capacity theories mentioned above involve cases in which the soil supporting the foundation is homogeneous and extends to a considerable depth. However, in practice, layered soil profiles are often encountered. For layered clayey soil, Button (1953) was the first to analyse footings on layered soils of different cohesion. Many other studies

Were conducted for clayey layers including those of Sivareddy and Srinivasan (1967) and Desai and Reese (1970). In another case, many authors studied the bearing capacity of a sand layer overlaying a clay layer. These studies were conducted by Meyerhof (1974), Meyerhof and Hanna (1978), Hanna and Meyerhof (1980), Hardy and Townsend (1982), Okamura *et at*. (1997), Kenny and Andrawes (1996), Burd and Frydman (1997), and Michalowski and Shi (1995).

Several important examples exist of foundation engineering problems in which it may be neces

sary to include the effect of soil layers in an assessment of bearing capacity. Shallow offshore foundations, for example, generally have large physical dimensions; potential failure surfaces may therefore extend a significant distance below the soil surface. Any soil layers within the depth of these failure surfaces would be expected to influence the failure load. Other examples include structures placed on engineered fill layers (e.g. oil storage tanks which may be founded on a thin layer of granular fill, and unpaved roads built on soft clays where a layer of compacted fill is used to spread the load applied by passing vehicles.

Attempts were made by researchers to use geosynthetics with subbase layers. There are several publications describing the influence of geosynthetics on increasing the soft-soil bearing capacity. Pospisil and Zednik (2003) dealt with clarifying the possible geosynthetics functionality. Six kinds of gesynthetics of world known producers were selected for the measurement. The results of static plate tests show that the contribution of the geosynthetics to the bearing capacity increase is very limited. A significant increase appears only in case of a very low bearing capacity subgrade covered by a 20 cm thick subbase layer reinforced by some geosynthetics. After the static part of the experiment, the Geotechnical

Laboratory Testing Field was equipped with a cyclic loader to simulate real traffic loading and tests for the evaluation of possible bearing capacity increase due to geosynthetics usage were repeated.

Individual series of testing varied in types of used geosynthetics and subbase layers thicknesses laid on geosynthetics (or directly on the subgrade in case of the geosyntetics-free testing space). The first series had thickness of the first subbase layer 20 cm and the second subbase layer 20 cm (i.e. 40 cm subbase layer in total). The second series of testing had thicknesses of the subbase layers 15 cm + 15 cm = 30 cm in total. The third, fourth and fifth series had the same thicknesses of subbase layers 20 cm + 10 cm = 30 cm in total.

The pre-described values of subgrade deformation modulus 5 MPa and 15 MPa for the 1st and 2nd testing series and for 3rd, 4th and 5th testing series respectively were achieved with difficulties by water content changing in the subsoil. The modulus was measured three times in each testing space. Values 5 MPa and 15 MPa are rounded off the average value (e.g. the minimum value was 5.75 MPa and the minimal value was 4.37 MPa in the first series).

The first subbase layer was spread just after subgrade modulus measurement because of the subsoil drying up. Subbase modulus of deformation was measured again three times in each testing spaces.

The test results of the five testing series are concentrated in Figure 1. In this place, it is necessary to highlight again that the thicknesses of subbase layers vary from series to series. They are 20 cm for both 1st and 2nd subbase layers in case of the 1st testing series, 15 cm in case of 2nd testing series and in case of 3rd, 4th and 5th series the 1st subbase layer was 20 cm and 2nd layer was 10 cm.

In this study, design charts are developed to help the designer choose the suitable thickness of granular (subbase) layer to be constructed over soft clay layers to maintain the design allowable bearing capacity.

Description of the Present Work

Engineers in Iraq used to construct a layer of granular (subbase) material below foundations. The thickness of this layer is selected arbitrarily between 0.3 m and 1.0 m. There is no scientific base for this selection. The layer consists of subbase class A or B according to the Iraqi Specifications and usually compacted by vibratory rollers to maintain a relative compaction of 95% according to the standard or modified Proctor compaction test.

In this work, four samples meeting the Iraqi specifications of subbase class B are selected and detailed laboratory tests are carried out on these samples. ASTM Test Designation (D-2049) (1999) provides a procedure for determining the minimum and maximum dry unit weights of granular soils so that they can be used to measure the relative density of compaction in the field. The relative density of each sample was determined by the following procedure:

1. The samples were first compacted in the mold of the standard Proctor compaction test following the specification of ASTM (D-698). Then 95% of the maximum dry unit weight is considered the field dry unit weight (γ_{dn}) since all subbase

layers are compacted in the field to this degree of compaction.

2. For a determination of the minimum dry unit weight, sand is loosely poured into the mold from a funnel with a 12.7 mm diameter spout. The average height of the fall of sand into the mold is maintained at about 25.4 mm.
3. The maximum dry unit weight is determined by vibrating sand in the mold for 8 min. A surcharge of 14 kN/m^2 (2 ib/in^2) is added to the top of the sand in the mold. The sample is vibrated in the mold. The value of (γ_{dmax}) can be determined at the end of the vibration with knowledge of the weight and volume of the sand.

Then the relative density of each sample was calculated as follows:

$$D_r = \frac{\gamma_{dn} - \gamma_{d\,\min.}}{\gamma_{d\,\max.} - \gamma_{d\,\min.}} \frac{\gamma_{d\,\max.}}{\gamma_{dn}} \quad \ldots (1)$$

The results of classification tests on the four samples of subbase class B are listed in Table 1 while the grain size distribution of the four samples is drawn in Figure 2. It can be noticed that the samples were compacted at a relative density ranging between 66% and 86%.

Bearing Capacity of Foundation on Layered $c - \phi$ Soil:

Stronger Soil Underlain by Weaker Soil

Meyerhof and Hanna (1978) developed a theory to estimate the ultimate bearing capacity of a shallow rough continuous foundation supported by a strong soil layer underlain by a weaker soil layer as shown in Figure 2. According to their theory, at ultimate load per unit area q_u, the failure surface in soil will be as shown in Figure 3. If the ratio H/B is relatively small, a punching shear failure will occur in the top (stronger) soil layer followed by a general shear failure in the bottom (weaker) layer. Considering the unit length of the continuous foundation, the ultimate bearing capacity can be given as (Das, 2009):

$$q_u = q_b + \frac{2(c_a + P_p \sin\delta)}{B} - \gamma_1 H \quad \ldots (2)$$

where: B = width of the foundation,

γ_1 = unit weight of the stronger soil layer,

Ca = adhesive force along aa' and bb',

Pp = passive force on faces aa' and bb',

q_b = bearing capacity of the bottom soil layer, and

δ = inclination of the passive force Pp with the horizontal.

$$C_a = c_a H \quad \ldots\ldots (3)$$

where c_a = unit adhesion.

$$q_p = \frac{1}{2}\gamma_1 H^2 \left(\frac{K_{pH}}{\cos\delta}\right) + (\gamma_1 D_f)(H)\left(\frac{K_{pH}}{\cos\delta}\right) = \frac{1}{2}\gamma_1 H^2 \left(1 + \frac{2D_f}{H}\right)\left(\frac{K_{pH}}{\cos\delta}\right) \quad \ldots (4)$$

where

K_{pH} = horizontal component of the passive earth pressure coefficient.

Also,

$$q_b = c_2 N_{c(2)} + \gamma_1 (D_f + H) N_{q(2)} + \frac{1}{2}\gamma_2 B N_{\gamma(2)}$$

…….. (5)

where

c_2 = cohesion of the bottom (weaker) layer of soil,

γ_2 = unit weight of bottom soil layer, and

Nc(2), Nq(2), Nγ(2) = bearing capacity factors for the bottom soil layer (that is, with respect to the soil friction angle of the bottom soil layer (2).

Combining equations (3), (4), and (5),

$$q_u = q_b + \frac{2 c_a H}{B} + 2\left[\frac{1}{2}\gamma_1 H^2\left(1+\frac{2D_f}{H}\right)\right]\left(\frac{K_{pH}}{\cos\delta}\right)\left(\frac{\sin\delta}{B}\right) - \gamma_1 H$$

$$= q_b + \frac{2c_a H}{B} + \gamma_1 H^2\left(1+\frac{2D_f}{H}\right)\frac{K_{pH}\tan\delta}{B} - \gamma_1 H$$

… (6)

Let $K_{pH}\tan\delta = K_s \tan\phi_1$

….. … (7)

where Ks = punching shear coefficient.

So,

$$q_u = q_b + \frac{2 c_a H}{B} + \gamma_1 H^2\left(1+\frac{2D_f}{H}\right)\frac{K_s \tan\phi_1}{B} - \gamma_1 H$$

…..… (8)

The punching shear coefficient can be determined using the passive earth pressure coefficient charts proposed by Caquot and Kerisel (1949). Figure 4 gives the variation of *Ks* with q_2/q_1 and ϕ_1. It is noticed that q_1 and q_2 are the ultimate bearing capacities of a continuous surface foundation of width *B* under vertical load on homogeneous beds of upper and lower soils, respectively, or

$$q_1 = c_1 N_{c(1)} + \frac{1}{2}\gamma_1 B N_{\gamma(1)}$$ …….. (9)

where

$Nc_{(1)}$, $N\gamma_{(1)}$ = bearing capacity factors corresponding to soil friction angle ϕ_1.

$$q_2 = c_2 N_{c(2)} + \frac{1}{2}\gamma_2 B N_{\gamma(2)}$$ .. (10)

If the height *H* is large compared to the width *B* (Figure 3), then the failure surface will be completely located in the upper stronger soil layer, as shown in Figure 5. In such a case, the upper limit for q_u will be of the following form:

$$q_u = q_t = c_1 N_{c(1)} + q N_{q(1)} + \frac{1}{2}\gamma_1 B N_{\gamma(1)}$$

…….. (11)

Hence, combining equations (8) and (11),

$$q_u = q_b + \frac{2 c_a H}{B} + \gamma_1 H^2 \left(1 + \frac{2 D_f}{H}\right) \frac{K_s \tan \phi_1}{B} - \gamma_1 H \le q_t$$

…….. (12)

For rectangular foundations, the preceding equation can be modified as:

$$q_u = q_b + \left(1 + \frac{B}{L}\right)\left(\frac{2 c_a H}{B}\right)\lambda_a + \left(1 + \frac{B}{L}\right)\gamma_1 H^2 \left(1 + \frac{2 D_f}{H}\right)\left(\frac{K_s \tan \phi_1}{B}\right)\lambda_s - \gamma_1 H \le q_t$$

…….. (13)

where λ_a, λ_s = shape factors.

$$q_b = c_2 N_{c(2)} \lambda_{cs(2)} + \gamma_1 (D_f + H) N_{q(2)} \lambda_{qs(2)} + \frac{1}{2} \gamma_2 B N_{\gamma(2)} \lambda_{\gamma s(2)}$$

.. (14)

$$q_t = c_1 N_{c(1)} \lambda_{cs(1)} + \gamma_1 D_f N_{q(1)} \lambda_{qs(1)} + \frac{1}{2} \gamma_1 B N_{\gamma(1)} \lambda_{\gamma s(1)}$$

……(15)

$\lambda cs_{(1)}$, $\lambda qs_{(1)}$, $\lambda \gamma s_{(1)}$ = shape factors for the top soil layer (friction angle = ϕ_1),

$\lambda cs_{(2)}$, $\lambda qs_{(2)}$, $\lambda \gamma s_{(2)}$ = shape factors for the bottom soil layer (friction angle = ϕ_2).

Based on the general equations [equations (13), (14), and (15)], some special cases may be developed. They are as follows:

Stronger Granular Layer over Weaker Saturated Clay (ϕ_2 = 0)

For this case, c_1 = 0; hence, c_a = 0. Also for ϕ_2 = 0, $Nc_{(2)}$ = 5.14, $N\gamma_{(2)}$ = 0, $Nq_{(2)}$ = 1, λcs = 1 + 0.2 (B/L), λqs = 1 (shape factors are Meyerhof's values). So,

$$q_u = 5.14 c_2 \left[1 + 0.2\left(\frac{B}{L}\right)\right] + \left(1 + \frac{B}{L}\right)\gamma_1 H^2 \left(1 + \frac{2 D_f}{H}\right)\left(\frac{K_s \tan \phi_1}{B}\right)\lambda_s - \gamma_1 D_f \le q_t$$

…. (16)

where

$$q_t = \gamma_1 D_f N_{q(1)} \left[1 + 0.1\left(\frac{B}{L}\right)\tan^2\left(45 + \frac{\phi_1}{2}\right)\right] + \frac{1}{2}\gamma_1 B N_{\gamma(1)} \left[1 + 0.1\left(\frac{B}{L}\right)\tan^2\left(45 + \frac{\phi_1}{2}\right)\right]$$

…….. (17)

In equation (17), the relationships for the shape factors λqs and λgs are those given by Meyerhof. Note that K_s is a function of q_2/q_1 [equations (9) and (10)]. For this case,

$$\frac{q_2}{q_1} = \frac{c_2 N_{c(2)}}{\frac{1}{2}\gamma_1 B N_{\gamma(1)}} = \frac{5.14 c_2}{0.5 \gamma_1 B N_{\gamma(1)}}$$

… (18)

Once q_2/q_1 is known, the magnitude of K_s can be obtained from Figure 4, which, in turn, can be used in equation (16) to determine the ultimate bearing capacity of the foundation q_u. The value of the shape factor λs for a strip foundation can be taken as one. As per the experimental work of Hanna and Meyerhof, the magnitude of λs appears to vary between 1.1 and 1.27 for square or circular foundations. For conservative designs, it may be taken as one.

Based on this concept, Hanna and Meyerhof (1980) developed some alternative design charts to determine the punching shear coefficient K_s, and these charts are shown in Figures 6 and 7. In order to use these charts, the ensuing steps need to be followed.

1. Determine q_2/q_1.
2. With known values of ϕ_1 and q_2/q_1, the magnitude of δ/ϕ_1 is determined from Figure 7.
3. With known values of ϕ_1, δ/ϕ_1, and c_2, K_s is determined from Figure 7.

Calculation of Subbase Layer Thickness for a Selected Bearing Capacity:

In this section, we will make use of equations (16) to (18) to calculate the bearing capacity of the subbase layer underneath by a soft clay layer. The angle of friction for the subbase material, ϕ_1 was estimated depending on the value of relative density using empirical relationship proposed by Rahardjo (2001). The soil layer above the foundation base level is assumed to be a backfill material of the same natural soft clay.

Figures (8) to (13) show the variation of the bearing capacity of the two-layer system with the thickness of subbase layer, H for different foundation geometries (B/L = 1, 0.8, 0.6, 0.4, 0.2, 0.0). The allowable bearing capacity q_a is calculated assuming a factor of safety of 2. It can be noticed that the bearing capacity increases linearly with H. As the ratio B/L decreases, the bearing capacity increases. This means that as the shape of the foundation is close to strip, it provides larger values of bearing capacity.

Subbase Type B , Relative Density =77.14%, D_f = 0.75 m

In order to obtain design charts easy for use in selection of the subbase layer thickness, a parametric study was carried out to study the effect of several parameters including: B/L, depth of footing D_f and the undrained cohesion of the soft clay layer c_2. For practical purposes, the subbase material is assumed to be compacted to a relative density of (77%) which is the average of the four values obtained experimentally.

Figures (14) to (19) are drawn for D_f = 0.75 m, while Figures (20) to (25) are for D_f = 1.0 m and Figures (26) to (31) are for D_f = 1.5 m. From these figures, the designers can selected the suitable thickness of the subbase layer for a design allowable bearing capacity.

It can be noticed that the relations are linear and that the rate of increase of the bearing capacity with the thickness of the subbase layer H is constant.

It can be concluded that when the cohesion of the clay layer is relatively large, ($c \approx 20$ or 25 kPa) and the depth of footing is suitable ($D_f \geq 1.0$ m), the required subbase layer is of small thickness (≤ 0.10 m). For practical

purposes and compaction requirements, it is suggested that the thickness H must not be less than 0.20 m.

Figures 14 to 31 can be used as design charts for selection of the adequate thickness of the subbase layer for a design value of bearing capacity.

Conclusions

The bearing capacity of subbase layer underneath by a soft clay layer is investigated. The properties of the subbase material are measured in the laboratory. Design charts were obtained which can be used to select the suitable thickness of the subbase layer for a design allowable bearing capacity.

It was concluded that when the cohesion of the clay layer is relatively large, ($c \approx 20$ or 25 kPa) and the depth of footing is suitable ($D_f \geq 1.0$ m), the required subbase layer is of small thickness (≤ 0.10 m). For practical purposes and compaction requirements, it is suggested that the thickness H must not be less than 0.20 m.

References

[1] American Society for Testing and Materials 1999. ASTM Standards, Vol. 0408, West Conshohocken, Pa.

[2]Burd, Hj. and S. Fridman. 1997. Bearing Capacity of Plane-Strain Footings on Layered Soils. Canadian Geotechnical Journal 34: pp. 241-253.

[3]Button, S.S., 1953, The Bearing Capacity of Footings on Two-Layer Cohesive Subsoil, Proceedings of the Third International Conference on Soil Mechanics and Foundation Engineering, 1: pp. 332-335.

[4]Caquot, A., and J. Kerisel. 1949. Tables for the calculation of passive pressure, active pressure, and bearing capacity of foundations. Paris: Gauthier-Villars.

[5]Das, B. M. 2009. Shallow Foundations Bearing Capacity and Settlement, second edition, Taylor & Francis Group, an informa business.

[6]Desai, C.S. and Reese, L., 1970, Ultimate Capacity of Circular Footings on Layered Soils, J Indian Nat. Soc. Soil Mechanics and Foundation Engineering, Vol. 96, (1): pp. 41-50.

[7]Hansen, J.B. 1970. A Revised and Extended Formula for Bearing Capacity. Geotechnical Institute Bulletin 28: Copenhagen.

[8]Hanna, A. M., and Meyerhof, G. G., 1980, Design Charts for Ultimate Bearing Capacity for Sands Overlying Clays, Canadian Geotechnical Journal, Vol. 17, No. 2, 300.

[9]Hardy, A.C. and Townsend, F.C., 1982, Preliminary Investigation of Bearing Capacity of Layered Soils By Centrifugal Modeling, pp. 20-24, Transportation Research Record 872.

[10]Kenny, Mj. and K.Z. Andrawes, 1996, The Bearing Capacity of Footings on a Sand Layer Overlying Soft Clay. Geotechnique 47 (2), pp. 339-345.

[11]Meyerhof, G.G. 1963. Some Recent Research on the Bearing Capacity of Foundations, Canadian Geotechnical Journal 1 (1), pp. 16-26.

[12]Meyerhof, G.G. 1974. Ultimate Bearing Capacity of Sand Overlying Clay, Canadian Geotechnical Journal 11**, (**2), pp. 224-229.

[13]Meyerhof, G. G., and Hanna, A. M, 1978, Ultimate Bearing Capacity of Foundations on Layered Soils under Inclined Load, Canadian Geotechnical Journal, Vol. 15, No.4, pp. 565.

[14]Michalowsrl, R.L. and Shi, L., 1995, Bearing Capacity of Footings over Two-Layer Foundation Soils, Journal of Geotechnical Engineering, ASCE 121 (5): pp. 421-428.

[15]Okamura, M., Takemura, J., Kimura, T., 1997, Centrifuge Model Tests Bearing Capacity and Deformation of Sand Layer Overlying Clay, Soils and Foundations, 37 (1), pp. 73-88.

[16]Pospisil, K. and Zednik, P., 2003, Geosynthetics Limitations for Bearing Capacity Increase, Report, Department of Infrastructure, CDV – Transport Research Centre, Brno, Czech Republic.

[17]Prandtl, L. 1921, Uber Die Eindringungsfestigkeit Plastisher Baustoffe Und Die Festigkeit Von Schneiden.I Zeitschrift Fur Angewandte Mathematik Und Mechanik, 1 (1), pp. 15-20.

[18]Rahardjo, P. P., 2001, In Conjunction With International Conference on In Sity Measurement of Soil Properties and Case Histories, Bali, Indonesia.

[19]Reisser, H. 1924, Zum Erddruckproblem. Proceedings, Frist International Conference on Applied Mechanics, pp. 295-311. Delft.

[20]Sivareddy, A. and R. J. Srinivasan, 1967, Bearing Capacity of Footings on Layered Clays.

[21]Terzaghi, K., 1943, Theoretical Soil Mechanics. Ew York: J. Wiley & Sons.

[22]Vesic, A. S., 1973. Analysis of Ultimate Loads of Shallow Foundations. Journal of the Soil Mechanics and Foundations Division, ASCE, Vol. 99, SM 8, pp. 45-73.

Table 1: Geotechnical properties of the subbase material.

Sample	1	2	3	4
Loose $\gamma_{dry\ min.}$ (kN/m^3)	19.30	18.30	18.80	19.10
Dense $\gamma_{dry\ max.}$ (kN/m^3)	22.16	20.90	22.00	22.09
γ_{dry}	21.43	20.49	21.187	20.96
Dr (%)	77.0	86.0	77.0	66.0
C.B.R (%)	39	42	44	42
SO_3 (%)	4.36	3.72	3.5	3.83
Gypsum Content (%)	9.3	8	7.5	8.25

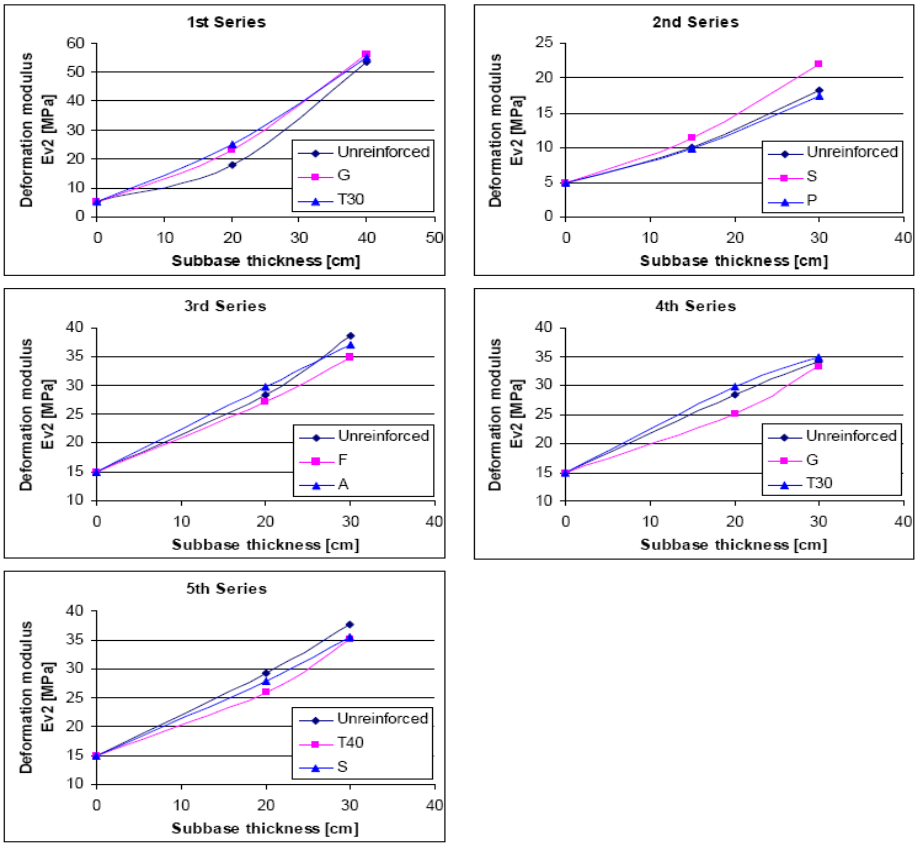

Figure 1: Test results of static tests of different geosynthetics reinforced subbase layers (Pospisil and Zednik, 2003).

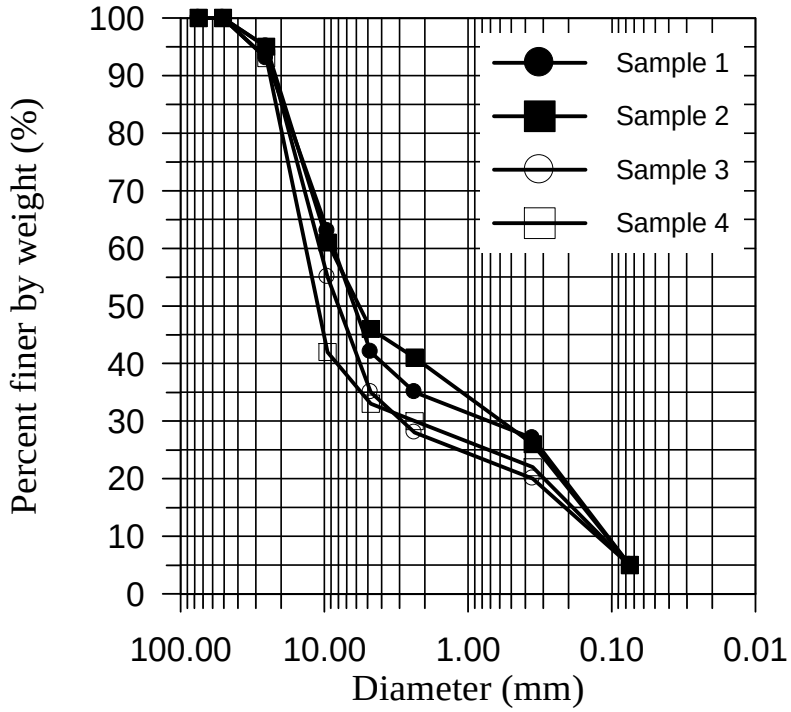

Figure 2: Grain size distribution of the four subbase samples.

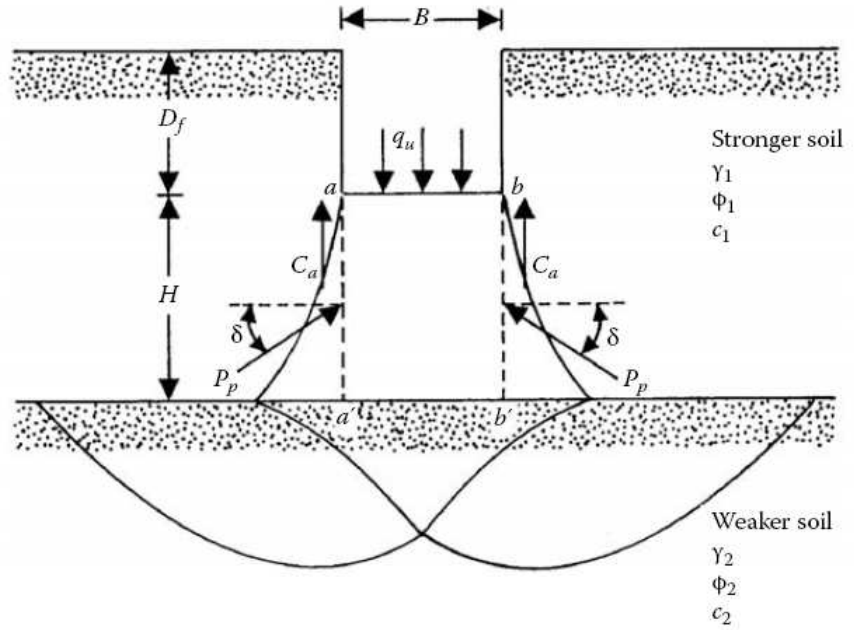

Figure 3: Rough continuous foundation on layered soil—stronger over weaker (from Das, 2009).

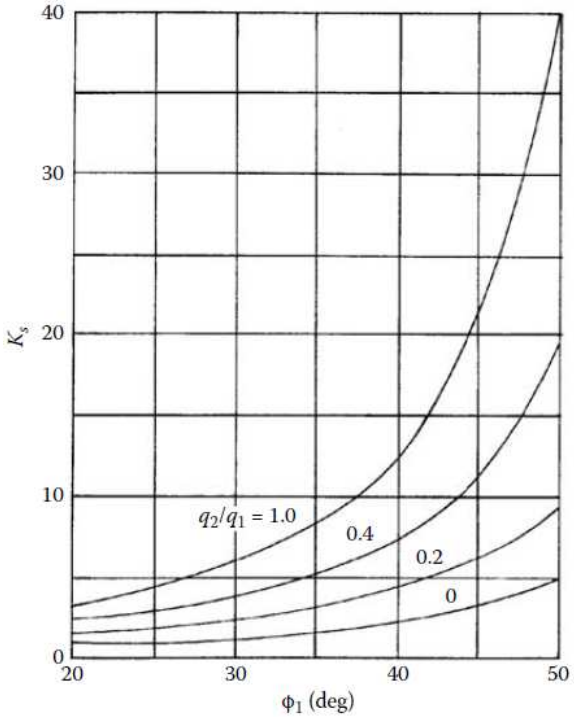

Figure 4 Meyerhof and Hanna's theory—variation of Ks with ϕ_1 and q_2/q_1 (from Das, 2009).

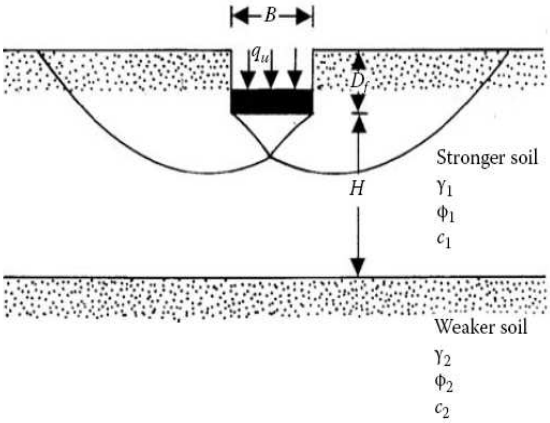

Figure 5 Continuous rough foundation on layered soil—*H*/*B* is relatively small (from Das, 2009).

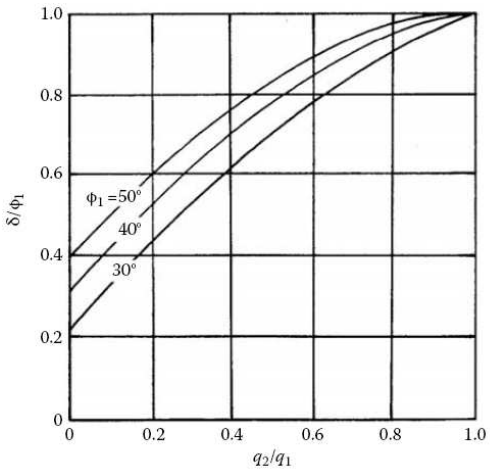

Figure 6 Hanna and Meyerhof's (1980) analysis—variation of δ/ϕ_1 with ϕ_1 and q_2/q_1—stronger sand over weaker clay.

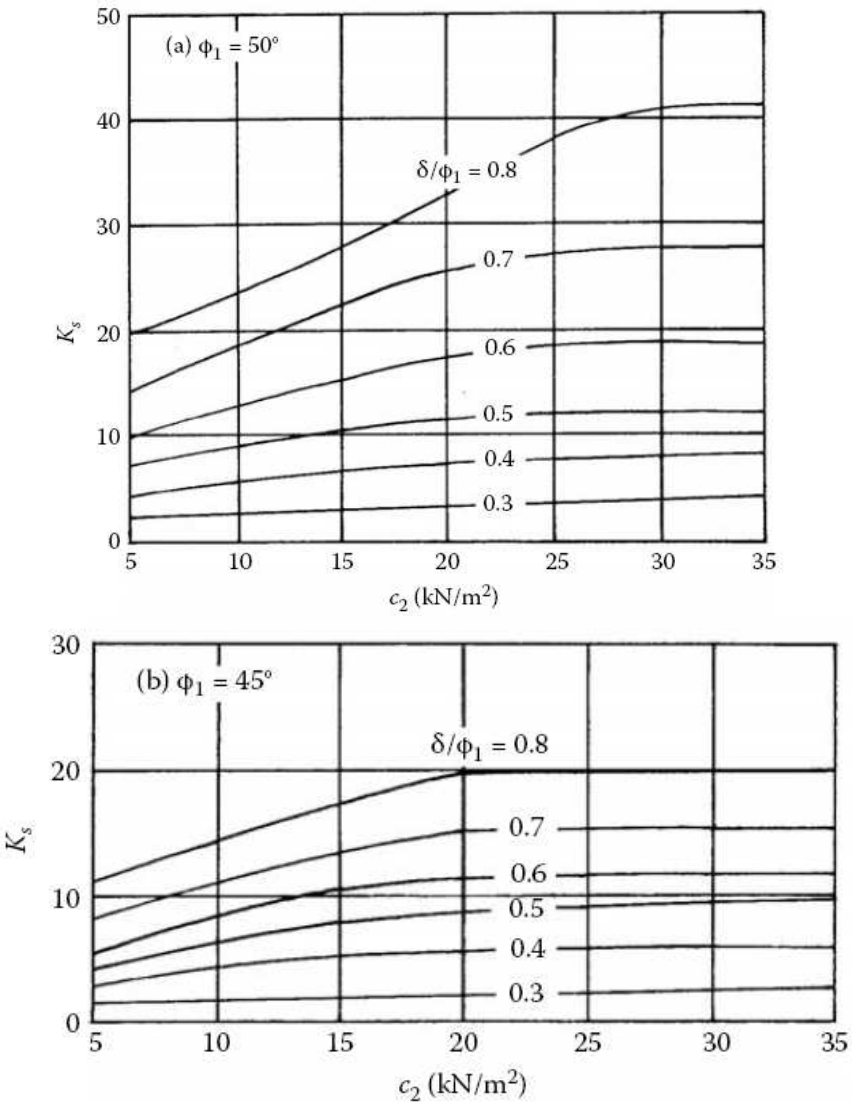
(a) $\phi_1 = 50°$
$\delta/\phi_1 = 0.8$
0.7
0.6
0.5
0.4
0.3
K_s
c_2 (kN/m^2)
(b) $\phi_1 = 45°$
$\delta/\phi_1 = 0.8$
0.7
0.6
0.5
0.4
0.3
K_s
c_2 (kN/m^2)

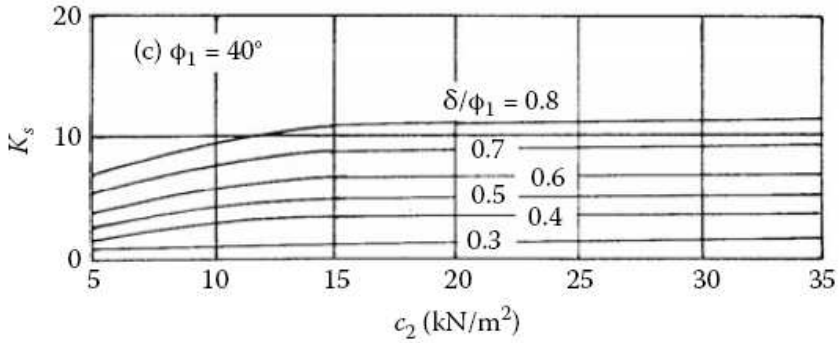

Figure 7 Hanna and Meyerhof's (1980) analysis for coefficient of punching shear—stronger sand over weaker clay.

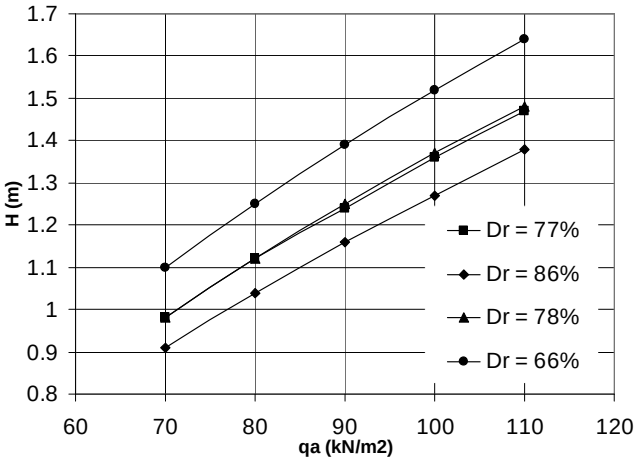

Figure 8 Effect of relative density on selection of the subbase layer thickness, D_f = 0.75 m, B/L = 0.

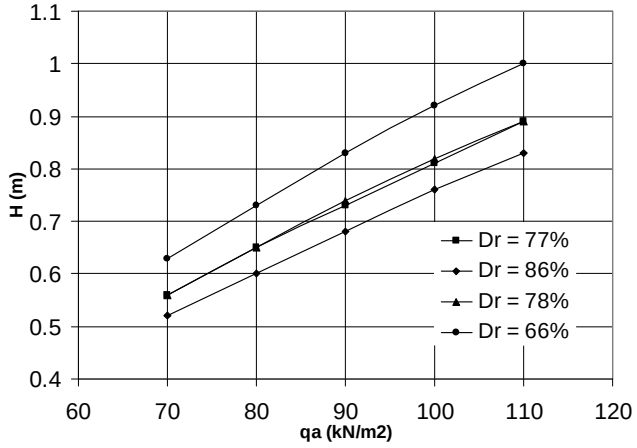

Figure 9 Effect of relative density on selection of the subbase layer thickness, D_f = 0.75 m, B/L = 1.

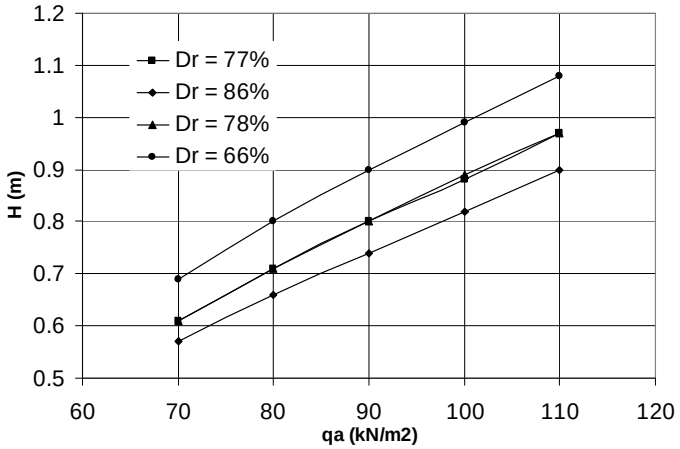

Figure 10 Effect of relative density on selection of the subbase layer thickness, D_f = 0.75 m, B/L = 0.8.

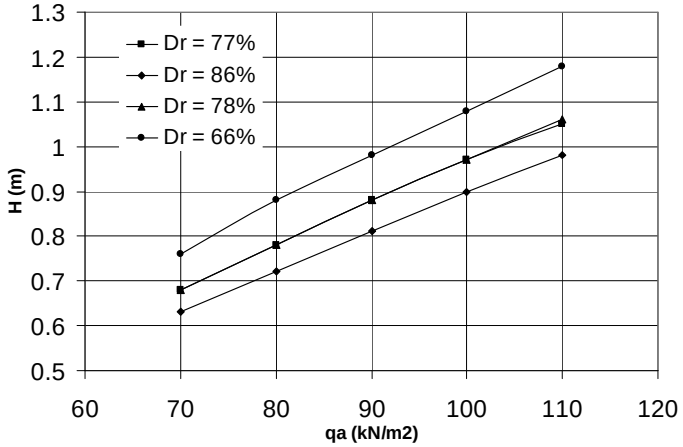

Figure 11 Effect of relative density on selection of the subbase layer thickness, D_f = 0.75 m, B/L = 0.6.

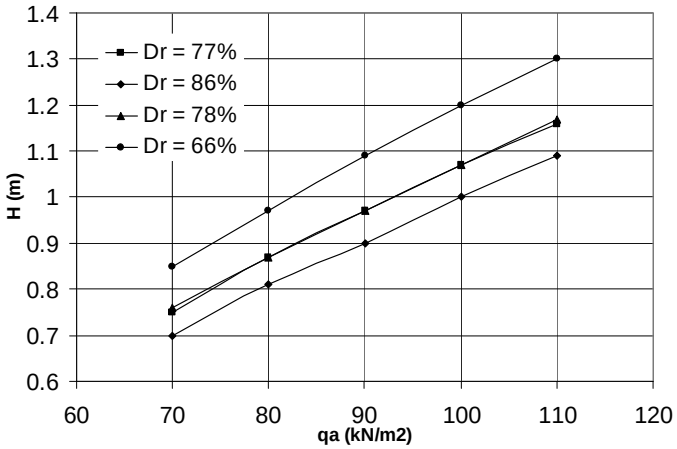

Figure 12 Effect of relative density on selection of the subbase layer thickness, D_f = 0.75 m, B/L = 0.4.

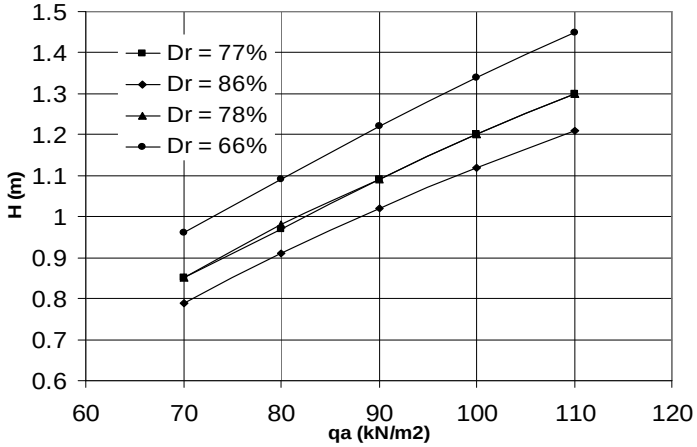

Figure 13 Effect of relative density on selection of the subbase layer thickness, D_f = 0.75 m, B/L = 0.2.

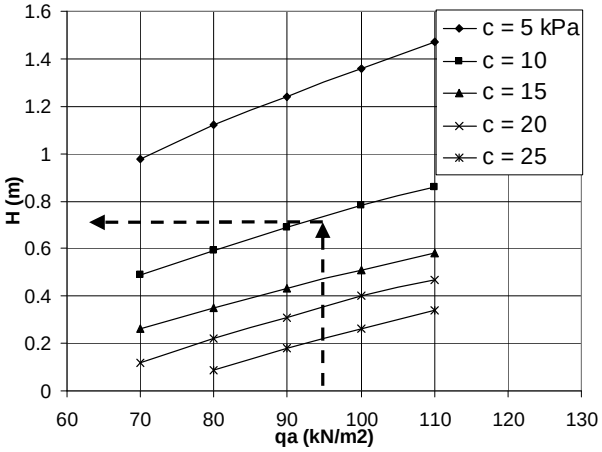

Figure 14 Design chart for selection the thickness of subbase layer, D_f = 0.75 m, B/L = 0.

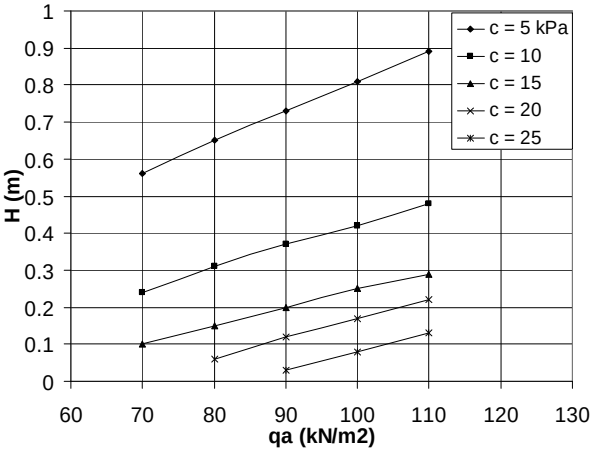

Figure 15 Design chart for selection the thickness of subbase layer, D_f = 0.75 m, B/L = 1.0.

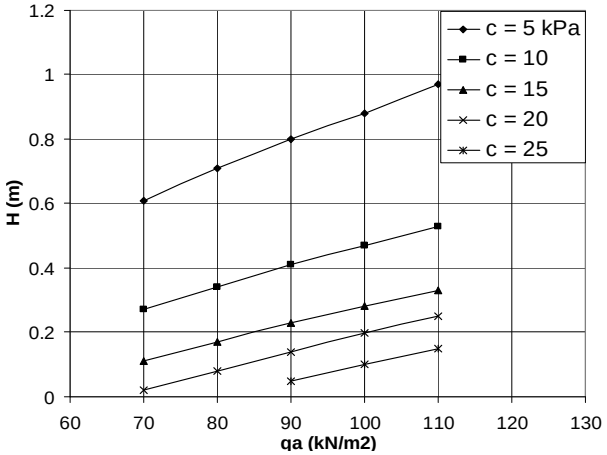

Figure 16 Design chart for selection the thickness of subbase layer, D_f = 0.75 m, B/L = 0.8.

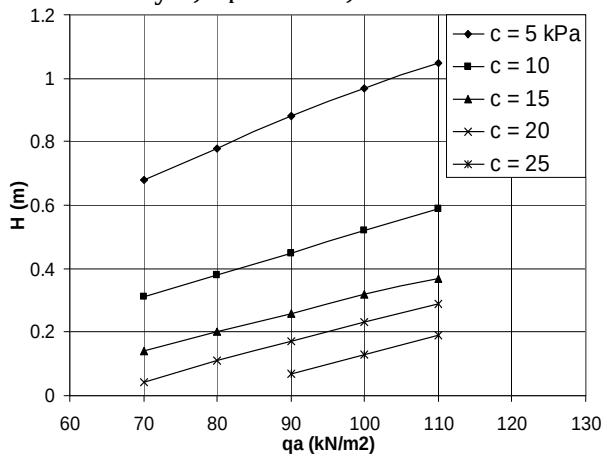

Figure 17 Design chart for selection the thickness of subbase layer, D_f = 0.75 m, B/L = 0.6.

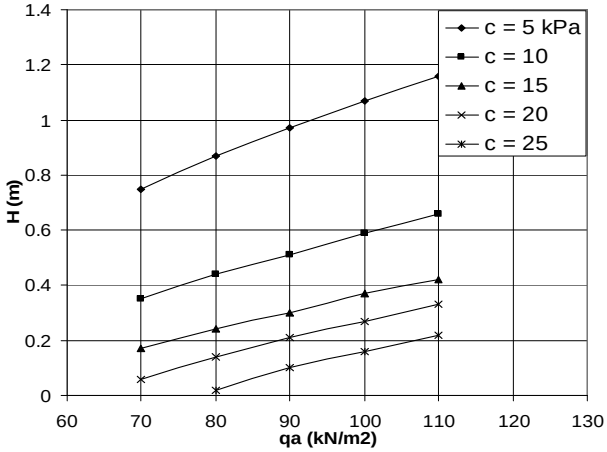

Figure 18 Design chart for selection the thickness of subbase layer, D_f = 0.75 m, B/L = 0.4.

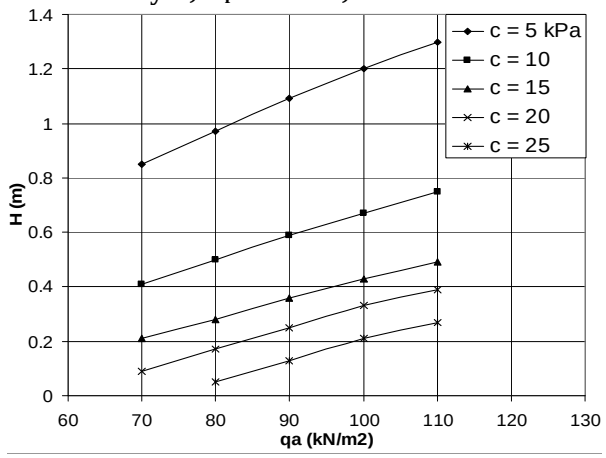

Figure 19 Design chart for selection the thickness of subbase layer, D_f = 0.75 m, B/L = 0.2.

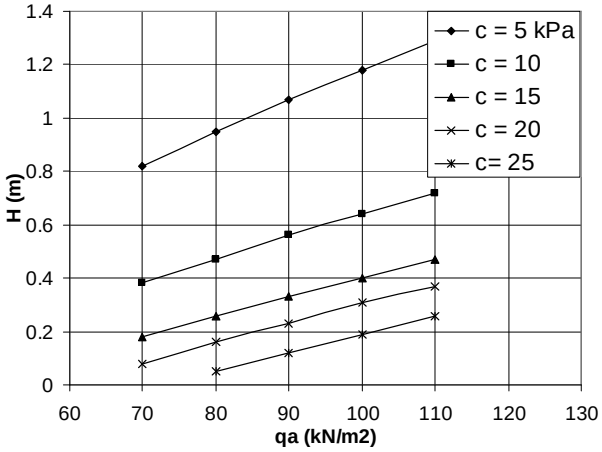

Figure 20 Design chart for selection the thickness of subbase layer, D_f = 1.0 m, B/L = 0.

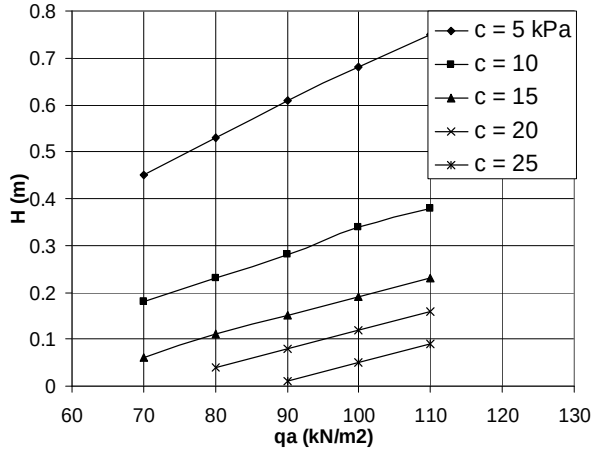

Figure 21 Design chart for selection the thickness of subbase layer, D_f = 1.0 m, B/L = 1.0.

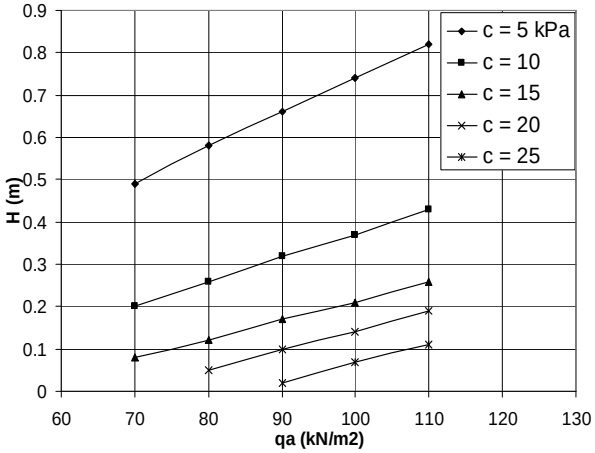

Figure 22 Design chart for selection the thickness of subbase layer, D_f = 1.0 m, B/L = 0.8.

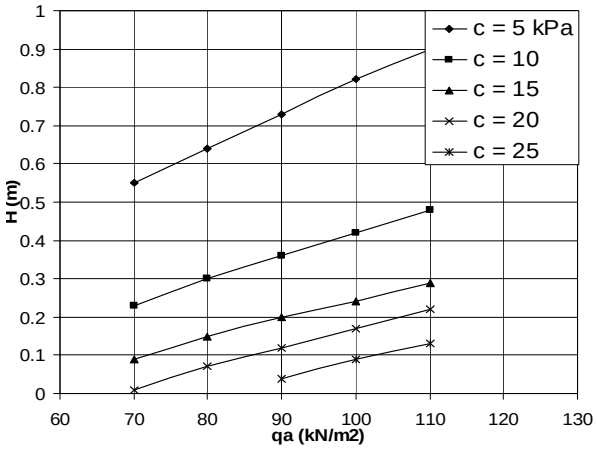

Figure 23 Design chart for selection the thickness of subbase layer, D_f = 1.0 m, B/L = 0.6.

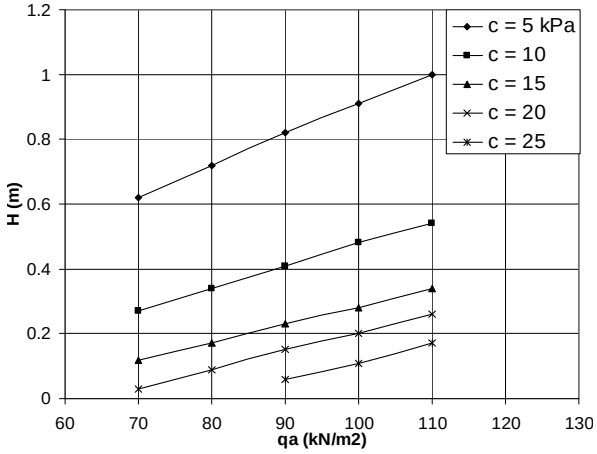

Figure 24 Design chart for selection the thickness of subbase layer, D_f = 1.0 m, B/L = 0.4.

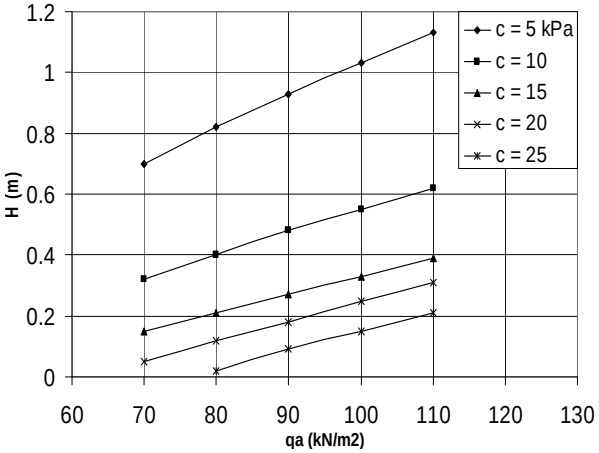

Figure 25 Design chart for selection the thickness of subbase layer, D_f = 1.0 m, B/L = 0.2.

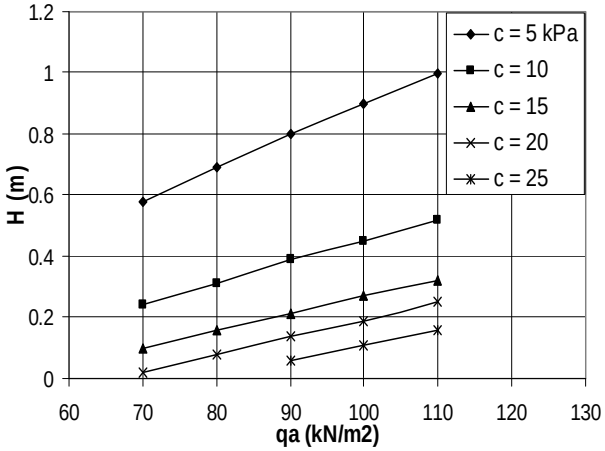

Figure 26 Design chart for selection the thickness of subbase layer , D_f = 1.5 m, B/L = 0.

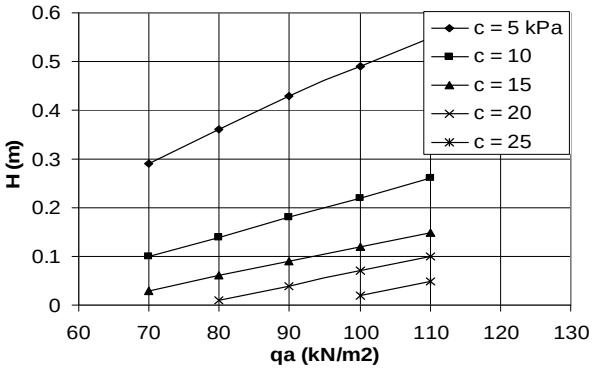

Figure 27 Design chart for selection the thickness of subbase layer, D_f = 1.5 m, B/L = 1.0.

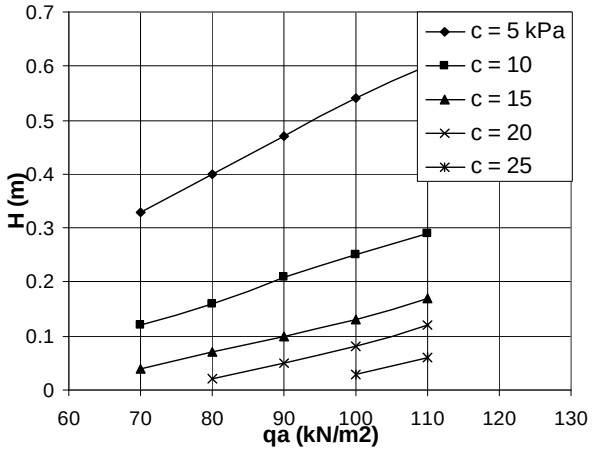

Figure 28 Design chart for selection the thickness of subbase layer,

D_f = 1.5 m, B/L = 0.8.

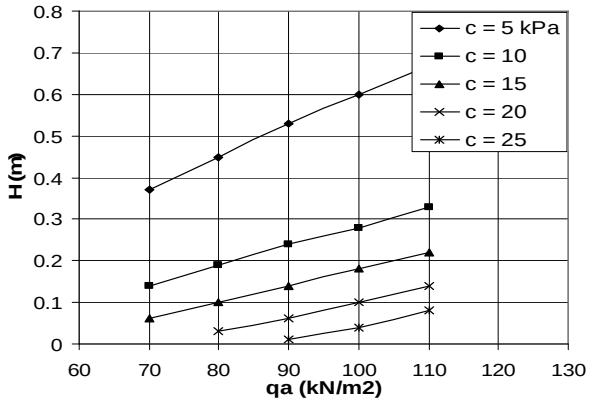

Figure 29 Design chart for selection the thickness of subbase layer, D_f = 1.5 m, B/L = 0.6.

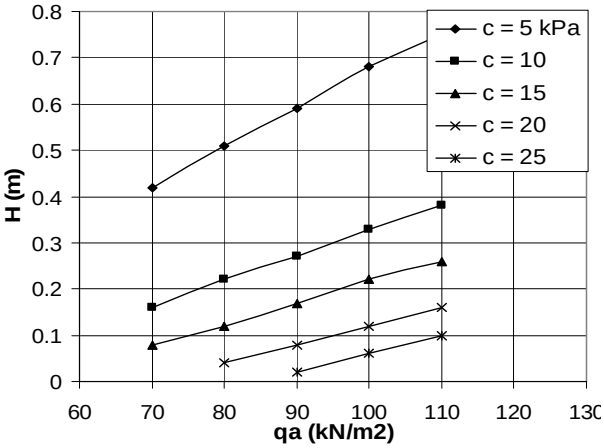

Figure 30 Design chart for selection the thickness of subbase layer, D_f = 1.5 m, B/L = 0.4.

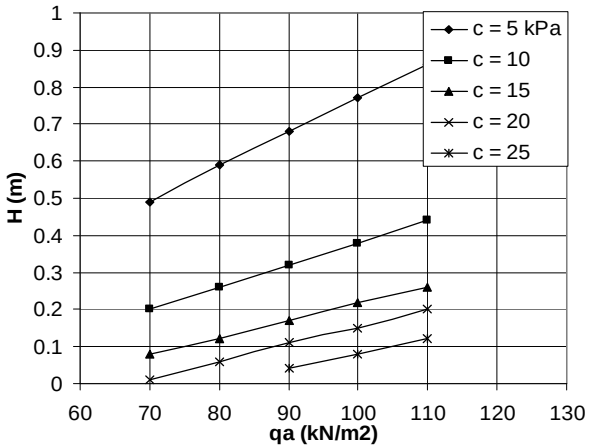

Figure 31 Design chart for selection the thickness of subbase layer, D_f = 1.5 m, B/L = 0.2.